# Schottky Barrier Receiver Modulator

By T. A. ABELE, A. J. ALBERTS, C. L. REN and G. A. TUCHEN

(Manuscript received January 26, 1968)

*This paper describes the receiver modulator of the TD-3 repeater. This modulator is a single-diode downconverter with an integral IF preamplifier. Its significant features are the use of a Schottky barrier diode, a waveguide directional filter, two lowpass filters for harmonic suppression, and image frequency absorption. The amplitude transmission characteristic of the modulator is flat to ±0.01 dB for ±6 MHz, and the average noise figure is 6.7 dB.*

## I. INTRODUCTION

The receiver modulator of the TD-3 repeater is the first unit in the signal path which uses active devices. Because it is in the signal path, its transmission characteristics must be well behaved, and because it is at the front end of the repeater, its low thermal noise is of considerable importance to the performance of the system.

## II. PERFORMANCE OBJECTIVES AND BASIC CONFIGURATION

### 2.1 *Objectives*

The objective of the development was to obtain a solid state downconverter-preamplifier for the microwave receiver of the TD-3 system. The unit had to be reliable, inexpensive, and in a shape to ease the transmitter-receiver bay designing. It should be easy to manufacture and maintain, and should have a minimum of adjustments. It should be designed to last at least 20 years and be rugged enough to withstand the shock and temperature extremes of shipment. In addition, it should conform to the following electrical specifications:

Signal midband frequency: $f_{SI}$ = 3710, 3730, . . . 4190 MHz, according to the frequency plan discussed in Ref. 1.

Local oscillator frequency: $f_{LO}$ = 3780, 3800, . . . 4120 MHz, according to the frequency plan discussed in Ref. 1.

Midband intermediate frequency: $f_{IF} = 70$ MHz.

Signal power: $P_{SI} = -28$ dBm nominally; for short hops, upfades and in anticipation of a possible increase of the transmitter output power, the design should be capable of operating satisfactorily with input signals as high as $P_{SI} = -19$ dBm.

Local oscillator power: $P_{LO} \leq 6$ dBm.

IF output power: $P_{IF} = 0$ dBm.

Signal to IF transmission: *Amplitude*—as flat as practicable; if possible within $\pm 0.005$ dB for $f_{SI} \pm 6$ MHz, $\pm 0.015$ dB for $f_{SI} \pm 10$ MHz; *Delay*—less than 0.1 ns distortion for $f_{SI} \pm 6$ MHz.

Noise figure: as low as possible, but less than 8 dB.

Signal input port: WR-229 waveguide.

Signal return loss: $RL_{SI} \geq 30$ dB for $f_{SI} \pm 10$ MHz.

Local oscillator input port: WR-229 waveguide.

Local oscillator return loss: $RL_{LO} \geq 10$ dB for $f_{LO}$.

IF output port: 75 Ω

IF output return loss: $RL_{IF} \geq 35$ dB for $f_{IF} \pm 10$ MHz.

Local oscillator suppression: local oscillator port (*i*) to signal port $\geq 35$ dB; (*ii*) to IF output port $\geq 50$ dB.

Local oscillator harmonics: The second and third harmonic of $f_{LO}$ shall each be at least 40 dB below $P_{LO}$ at the signal port and at the local oscillator port.

RF leakage: comparable to a good waveguide flange joint.

Temperature range: 75°F ±10°F nominally, but operative from 40° to 140°F.

Bias voltage: −19 V to ground.

Diode bias current monitoring meter: 20μA (5900Ω).

All of these requirements were met by the final design. However, the amplitude transmission characteristic from signal to IF is slightly more sensitive to temperature within the 75°F ±10°F temperature range than ideally desirable, but this is not expected to noticeably impair the performance of the system.

### 2.2 *Basic Design Considerations*

Four basic considerations and resulting decisions significantly influenced the design of the downconverter-preamplifier unit.

(*i*) A Schottky barrier diode was chosen because it appeared able to yield the required low noise figure.

(*ii*) A single diode was used, that is, an unbalanced downconverter was developed. The major advantages of such a converter are that

the cost of diodes for the converter is lowered by at least 50 per cent since a matched pair of diodes is not required; the diode can be biased externally, regardless of the polarity of the supply voltage, for example, only a negative voltage to ground is available in TD-3; and the connection to the IF preamplifier is simple and does not require a balanced transformer.

The noise performance of this downconverter should be comparable with its balanced counterpart, even though the unbalanced downconverter does not cancel the noise bands centered around $f = 0$ generated by local oscillator noise beating with the local oscillator carrier. However, this lack of noise suppression is of no consequence for most radio systems because the local oscillator power generally passes through a narrow bandpass filter so that no significant noise energy is contained in frequency regions $\pm 70$ MHz away from the local oscillator carrier. Appendix A gives a more detailed analysis of the noise performance of a balanced and an unbalanced downconverter using a simple model for the diode.

(*iii*) The power generated in the downconverter at the image frequency band is absorbed rather than reflected to the diode with a suitable phase shift. As is well known, reflecting the power would raise the efficiency of the conversion process and hence lower the noise figure. It was estimated from preliminary investigations that the penalty in noise figure for absorbing the image power is approximately 0.7 dB. This appeared to be a fair price for the advantages gained. Since in absorbing the image power, for example, in an isolator, no narrowband reactance has to be placed into the path of the signal, there is a better chance that the very stringent requirements pertaining to the amplitude and delay response of the downconverter can be met. Furthermore, no adjustment of an image reflecting reactive circuit is required.

(*iv*) Since difficulties often have been encountered from harmonics and harmonic sidebands of the local oscillator frequency originating in the diode, the diode was placed between two lowpass filters. This not only assures that the level of harmonics emanating from the downconverter is drastically reduced; it is very unlikely that the impedances of the connecting circuits at the harmonic frequencies will influence the performance of the downconverter appreciably. This is quite important, since these impedances are usually not under control.

These four basic decisions lead to the block diagram shown in Fig.

1. The signal power and the local oscillator power are combined in the adding network and pass to the diode through the isolator and the first lowpass filter. The cutoff frequency of this lowpass filter is at approximately 1.5 × (average local oscillator frequency) so that it passes the local oscillator frequency and the signal and image band of all channels without any appreciable attenuation, and that it stops all undesirable harmonics and harmonic sidebands of the local oscillator frequency present at the diode.

The isolator has broadband characteristics so that it passes the signal band and the local oscillator frequency in the forward direction and absorbs these frequencies as well as the image band in the reverse direction. It also makes the return loss at the signal and local oscillator port virtually independent of the diode properties.

The intermediate frequency generated in the diode passes through the second lowpass filter, is amplified in the preamplifier and appears at the IF output port. The dc-bias is derived from the −19 V available in the preamplifier and is fed to the diode from the preamplifier through the second lowpass filter. The cutoff frequency of this lowpass filter is at approximately 0.5 × (average local oscillator frequency) so that it passes the dc-bias and the IF band without any appreciable attenuation, and that it attenuates all undesirable microwave frequencies present at the diode.

It was decided to realize the combination of the lowpass filter, the diode mount, and the second lowpass filter as a waveguide-coaxial structure. It appeared then that a very suitable realization for the adding network would be a waveguide directional filter of the type

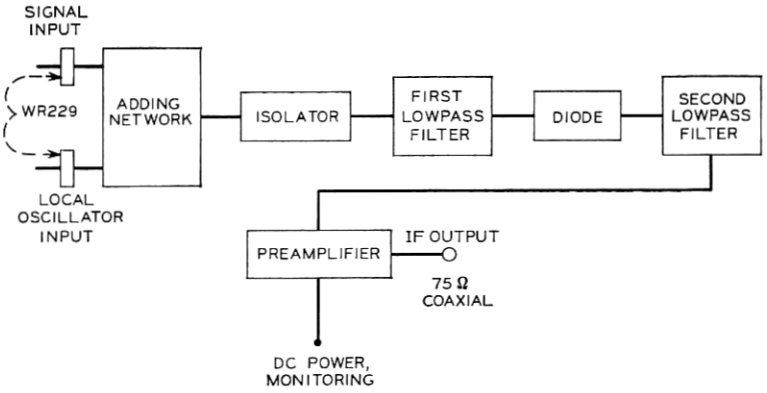


Fig. 1 — Basic downconverter-preamplifier block diagram.

described in Ref. 2. Since any filter is most sensitive to manufacturing deviations and environmental conditions around the frequency where its resonators resonate, it was decided to pass the local oscillator frequency through the bandpass section of the directional filter and the signal band through the bandstop section. Thus, all resonators of the directional filter resonate at the local oscillator frequency, and the response of the filter at the signal band is rather insensitive to manufacturing deviations and environmental conditions. The resulting block diagram is shown in Fig. 2.

Although the location of the isolator in Fig. 2 is ideal from the viewpoint of the downconverter design, it was necessary to move the isolator to the signal input port to avoid multiple reflections between the bandstop section of the directional filter and the channel bandpass filter which precedes the downconverter.[1] Therefore, the configuration shown in Fig. 3 was finally adopted.

A block not in Fig. 2 is the step transducer between the directional filter and the first lowpass filter. This transducer is necessary because the first lowpass filter requires reduced height waveguide as the connecting waveguide. This lowpass filter must be a multimode lowpass filter, that is, it must stop harmonics and harmonic sidebands of the local oscillator frequency generated in the diode irrespective of the mode in which they occur. The only known solution for this requirement is the "waffle iron filter,"[3] which must be operated between reduced height guides. No transducer is required between the first lowpass filter and the diode because initial estimates indicated that

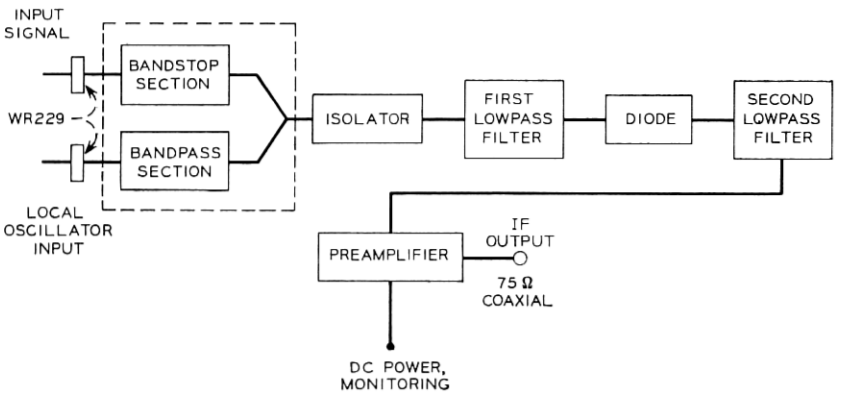


Fig. 2 — Detailed downconverter-preamplifier block diagram.

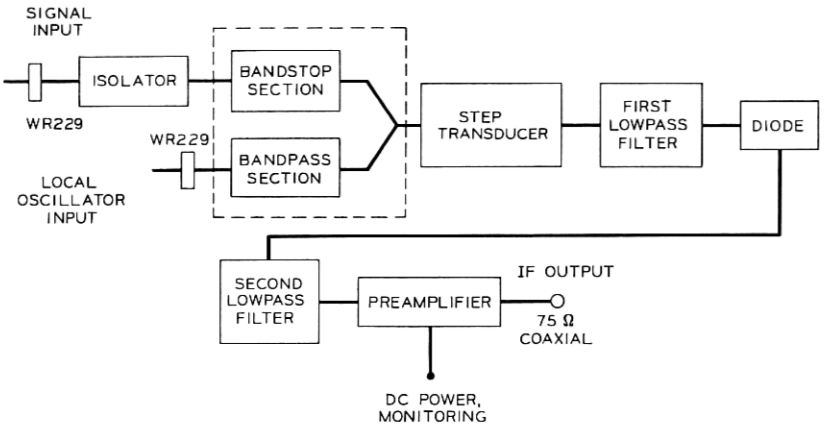


Fig. 3 — Final downconverter-preamplifier block diagram.

the Schottky barrier diode could be operated quite well in a reduced height waveguide.

## III. DETAILED ELECTRICAL DESIGN

### 3.1 *Directional Filter*

The structure, the properties and the design of the kind of waveguide directional filter used for this downconverter are described in Ref. 2. Therefore this discussion is confined to establishing the requirements, deciding the values of $n$ (number of bandpass and bandstop cavities) and $Q_T$ (selectivity factor) of the filter, and presenting the actual results obtained.

Fig. 4 is a sketch of the directional filter for $n=2$. As a result of the requirements discussed in Section 2, the following requirements were imposed on the directional filter:

Midband frequency: $f_{LO}$.

Transmission from port 3 to port 1: *Amplitude*—Flat to within $\pm 0.005$ dB for the two 12 MHz bands centered at $f_{LO} \pm 70$ MHz and flat to within $\pm 0.015$ dB for the two 20 MHz bands centered at $f_{LO} \pm 70$ MHz; *Delay*—Less than 0.1 ns distortion for the two 12 MHz bands centered at $f_{LO} \pm 70$ MHz.

Insertion loss at $f_{LO}$ from port 2 to port 3: $\geq$ 5 dB. (The isolator provides another 30 dB.)

Return loss at port 1: $\geq$ 30 dB for the two 20 MHz bands centered at $f_{LO} \pm 70$ MHz.

Return loss at port 2: $\geq$ 20 dB at $f_{LO}$.

Return loss at port 3: $\geq$ 30 dB for the two 20 MHz bands centered at $f_{LO} \pm 70$ MHz.

Ports: WR-229 waveguide.

Temperature range: 75°F ±10°F but operative from 40° to 140°F.

It is obvious from these requirements that the $Q_T$ of the filter should be made as high as possible in order to meet the specifications with the smallest possible $n$.[2] The limiting factor in this connection is the dissipation loss in the filter, which reduces the insertion loss from port 2 to port 3 and raises the insertion loss from port 2 to port 1, as $Q_T$ is increased for a given $n$. For this reason $n = 1$ could not be used since it would require too high a $Q_T$. Consequently:

$$n = 2 \tag{1}$$

$$Q_T = 140 \tag{2}$$

were chosen since $Q_T \approx 150$ is known to be a reasonable upper limit.

The results obtained from a typical filter designed to these specifications are as follows:

Return loss at ports 1 and 2 as Fig. 5 shows.

Return loss at port 3: $\geq$ 40 dB for the two 60 MHz bands centered at $f_{LO} \pm 70$ MHz.

Insertion loss from port 2 port 3 as Fig. 6 shows.

Transmission from port 3 to port 1: *Amplitude*—At $f_{LO} \pm 70$ MHz, the insertion loss is 0.005 dB; for the two 20 MHz bands centered at $f_{LO} \pm 70$ MHz, the insertion loss is flat to within less than ±0.01 dB; *Delay*—It can be computed that the distortion will be a slope of 0.084 ns per 12 MHz for the two 12 MHz bands centered at $f_{LO} \pm 70$ MHz.

The insertion loss from port 2 to port 1 at $f_{LO}$ was measured to be typically 0.3 dB. In contrast with the other microwave filters of the TD-3 system,[4] it was decided to fabricate this filter out of copper instead

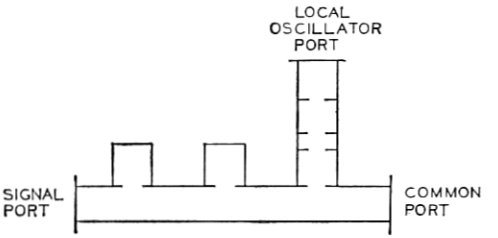


Fig. 4 — Directional filter. (Common: port 1, local oscillator: port 2, signal: port 3.)

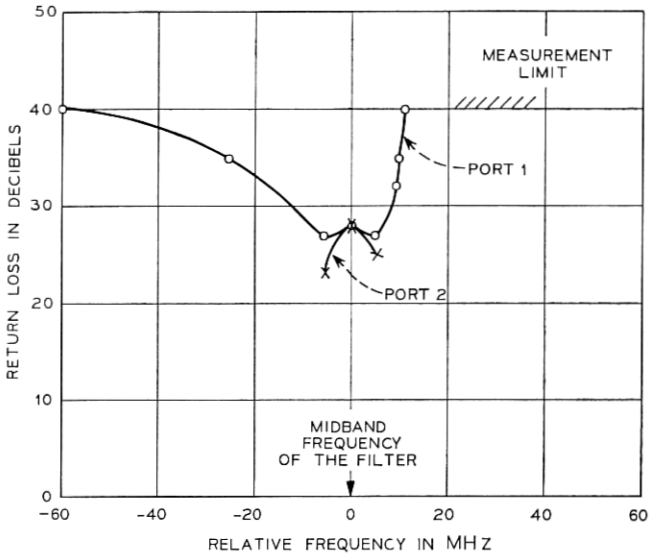


Fig. 5 — Return loss of ports 1 and 2 of the directional filter.

of copper-clad Invar, since it is apparent from the requirements that the frequency shift caused by changes in temperature and relative humidity can be tolerated.

### 3.2 *Converter Block*

The following general approach was used in designing the converter block consisting of the step transducer, the first and second lowpass filter, and the diode section:

(*i*) The dimensions of the converter block were experimentally determined in such a way that a *broadband* match was obtained at the microwave input port to the WR-229 waveguide (Fig. 7). This broadband match was obtained using local oscillator power levels of $P_{LO} = 0$, 3, and 6 dBm (maximum level available) and reasonable forward diode bias currents from 4 to 12 mA. No mechanical adjustment was required for any fixed $P_{LO}$ to obtain this match for all diodes and around all local oscillator frequencies. However, some adjustment of the bias current for different diodes and different local oscillator frequencies was required. It was assumed that the converter block designed by this procedure will behave approximately like a

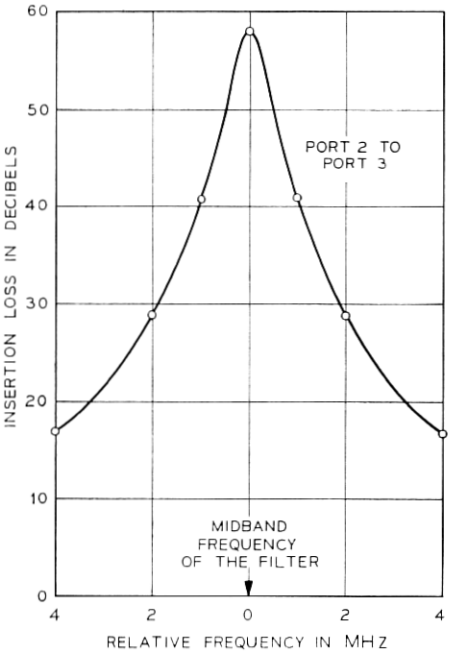


Fig. 6 — Insertion loss between ports 2 and 3 of the directional filter.

nonlinear conductance (that is, real admittance), when operated as a downconverter with the pertinent $f_{LO}$ and at an intermediate frequency of 70 MHz, for two reasons: (1) The broadband match indicates that the diode and diode mounting reactances have been successfully tuned out around the pertinent $f_{LO}$. (2) These reactances do not play any significant role at frequencies around 70 MHz and, similarly, the second lowpass filter does not provide any additional reactances because its cutoff frequency is well above 70 MHz, and its electrical length is short compared with the wavelength.

(*ii*) As a consequence of this, it can be expected that the converter block, after being adjusted with the bias current for an optimum

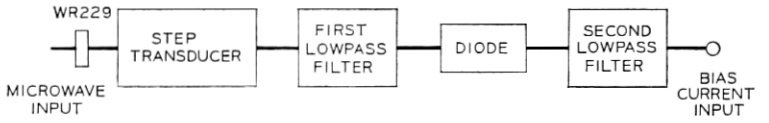


Fig. 7 — Block diagram of the converter block.

match at the pertinent $f_{LO}$ and when connected to form a downconverter as shown in Fig. 8, exhibits an IF output impedance $Z_{IFout}$, which is approximately real and constant over the band from 60 to 80 MHz.

(*iii*) For the same reason, this downconverter, when operated as shown in Fig. 9, can be expected to exhibit a signal to IF transmission characteristic with virtually no amplitude or delay distortion for the two 20 MHz bands centered around $f_{LO}$ ±70 MHz and to yield a conversion loss, defined as

$$CL/\text{dB} = 10 \lg P_{SI}/P_{IF}, \tag{3}$$

between 3 dB and 5 dB.[5] $P_{SI}$ is the incident signal power at the signal input port, and $P_{IF}$ is the IF power absorbed by the IF load $R_{IF}$ in Fig. 9. This load shall be a constant real resistance approximately equal to $Z_{IFout}$ in order to extract the available IF power from the converter.

(*iv*) Assuming that the input impedance of the IF preamplifier is made approximately equal to $R_{IF}$ and that the noise figure in dB of the IF preamplifier when measured from $R_{IF}$ is equal to $NF_{IF}$, the total single sideband noise figure $NF_{Total}$ in dB of the complete downconverter-preamplifier unit (Fig. 3) referred to a signal generator matched to the WR-229 waveguide can then be estimated to be:[5]

$$NF_{Total} = CL + NF_{IF} + 10 \lg \left(1 + \frac{1 - \frac{1}{2}10^{CL/10\,\text{dB}}}{10^{(CL+NF_{IF})/10\,\text{dB}}}\right)$$
$$\leqq CL + NF_{IF} \tag{4}$$

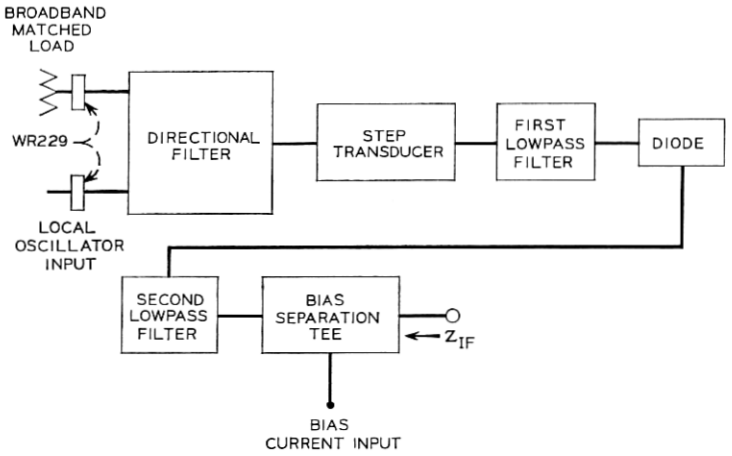


Fig. 8 — IF output impedance of the downconverter.

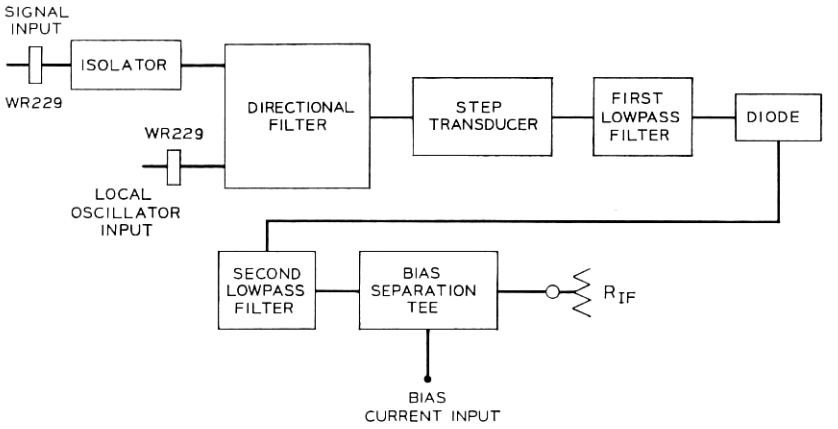


Fig. 9 — Block diagram of the downconverter.

Since $NF_{IF}$ is about 3 dB, the performance objective of $NF_{Total} < 8$ dB should be attainable.

The physical configuration chosen for the converter block is shown in cross section in Fig. 10.

The step transducer is a conventional[6] quarter wavelength transducer connecting from a height of 1.145 to 0.100 inch at a constant width of 2.29 in. It has three steps and provides a return loss of better than 22 dB from 3700 to 4200 MHz, which is entirely satisfactory for this application. The height of 0.100 in was chosen, since it is a convenient connecting height for the first lowpass filter, and was estimated to be a suitable height to obtain the desired broadband match of the diode to the local oscillator power.

The first lowpass filter is designed as a waffle iron filter, as explained in Section 2.2, based on a modification of a published design.[7] The number of sections was reduced to four and the design scaled according to the ratio of the waveguide widths. Judging from the published data, this should result in an insertion loss of at least 27 dB for a $TE_{10}$ mode from 6 to 16 GHz. The return loss from 3700 to 4200 MHz was measured between 2.29 × 0.1-inch rectangular waveguides to be better than 14 dB, which is satisfactory in this application.

No attempt was made to measure the multimode stopband insertion loss because of the formidable problems of such a measurement. It was established later, however, by measurements of the level of

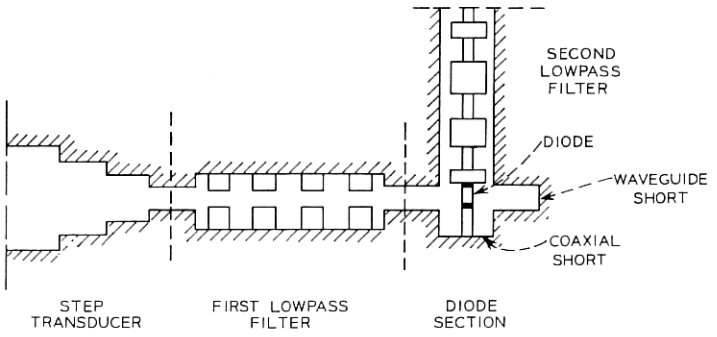


Fig. 10 — Cross section of the converter block.

harmonics of the local oscillator frequency emanating from the converter, that the rejection at these frequencies is adequate. Section 5.7 gives the results.

The second lowpass filter is a conventional stepped-impedance coaxial lowpass filter designed according to image parameter theory.[8] It has three sections, its outer conductor has a 0.288 inch diameter, and it starts with a low impedance line. The image cutoff frequency is 2460 MHz, and the filter is designed to furnish better than 40 dB of image attenuation from 3.7 GHz to at least 8.4 GHz. The image impedance at $f=0$ is 40Ω, resulting in virtually the same image impedance across the entire 60 to 80 MHz band. The value of 40Ω represents a compromise between manufacturing cost of the center conductor and electrical requirements. Since $Z_{IFout}$ turned out to be approximately 50Ω, an image impedance of 50Ω at $f=0$ would have been ideal. This, however, would have resulted in a rather thin center conductor in the high impedance lines of the filter. The electrical performance of the filter was not measured independently because the design procedure is sufficiently accurate and the filter in the down-converter performs satisfactorily (see Section 5.7).

The diode section is a 2.29 × 0.1-inch rectangular waveguide shorted at one end ("waveguide short" in Fig. 10). The diode is located in the center of the waveguide across the narrow dimension between the second lowpass filter and a shorted section ("coaxial short" in Fig. 10) of 30Ω coaxial line (which has an outer diameter of 0.288 inch).

The three available degrees of freedom—the distance between the diode and the waveguide short, the distance between the diode and

the first lowpass filter, and the length of the coaxial short—were determined empirically to yield the desired broadband match of the converter block to the local oscillator power. The dimensions arrived at are 0.250, 0.350, and 0.060 inch, respectively. These dimensions are valid for $P_{LO} = 6$ dBm (maximum power available), which was found to yield the lowest value for $CL$. The diode used is the Western Electric Company 497A gallium arsenide Schottky barrier diode.[9] (The equipment described in this article is manufactured by the Western Electric Company for Bell System use only.)

### 3.3 *Remaining Components*

The remaining components shown in Fig. 3 are the isolator and the IF preamplifier. Ref. 10 describes the preamplifier. The Western Electric Company 8A isolator was chosen because it has adequate broad band characteristics so that a single code covers all 24 signal midband frequencies with their associated local oscillator frequencies and image bands.

## IV. MECHANICAL DESIGN

The downconverter was designed very carefully to achieve a satisfactory compromise between the electrical requirements of high performance and reliability and the economic demands of low cost and easy manufacture. Starting with the basic arrangement of Fig. 11, it was decided to integrate the step transducer, waffle iron filter, and diode cavity into a single die-cast structure; the bandpass and bandstop filters were combined into the directional filter; the mounting on one side of the diode was integrated with the coaxial lowpass filter

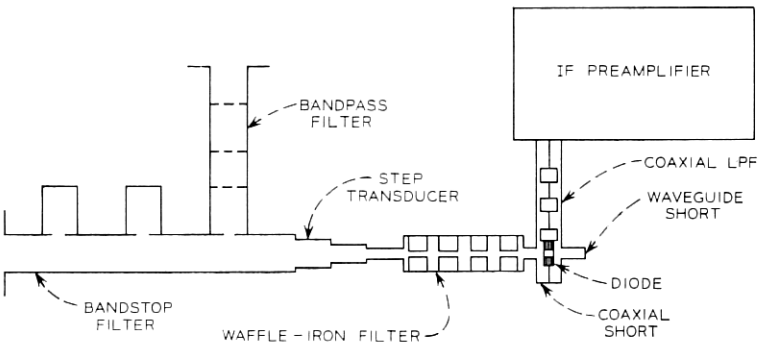


Fig. 11 — Basic arrangement of the downconverter-preamplifier assembly.

and on the other side with the coaxial short. It was recognized that particular effort would have to be devoted to the diode mounting in the final design. N-type connectors between the coaxial LPF and the IF preamplifier were helpful during early development but unnecessary in production.

The unit thus consists of six basic mechanical modules: directional filter, die-cast housing, collet assembly, diode, coaxial LPF, and IF preamplifier. Figure 12 shows the two halves of the die-cast housing, the collet assembly, the diode, and the coaxial LPF, and Fig. 13 shows a preproduction model of the entire unit. During final assembly, the modules are joined by screws, and two ¼-inch-long wire straps are added to connect the outer and inner conductor of the LPF to the IF preamplifier.

### 4.1 *The Directional Filter*

Figure 4 is a sketch of the directional filter. It shows the location of the two-cavity bandstop filter and the two-cavity bandpass filter. Both filters are channel-frequency dependent, and their resonance cavities require high-conductivity walls to reduce losses. These properties separate the directional filter sufficiently from the other components to make it a separate module. Either type of filter is traditionally made from sections of standard copper waveguide.

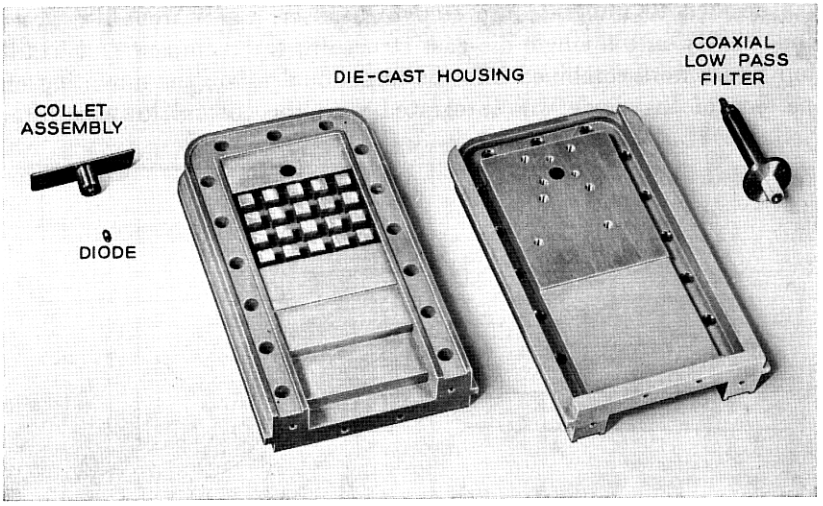


Fig. 12 — Four of the six mechanical modules.

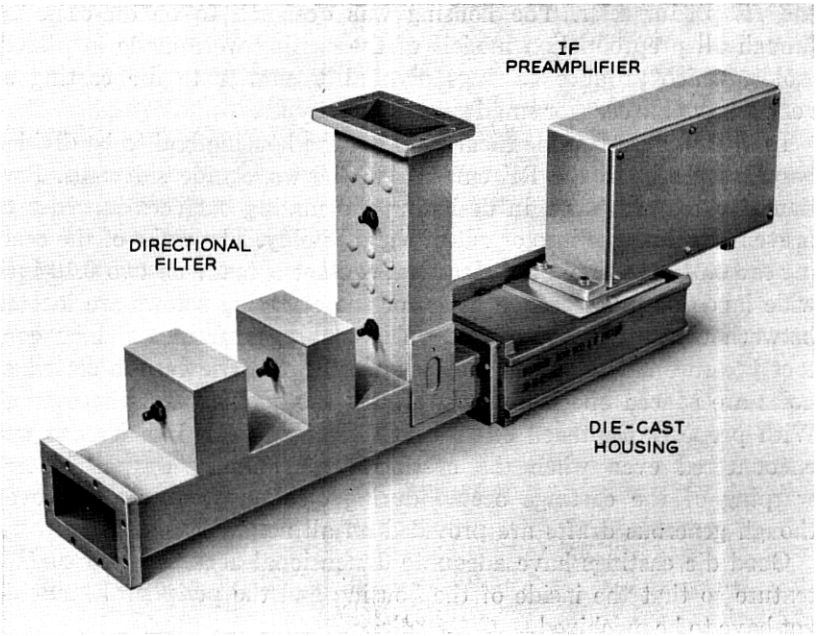


Fig. 13 — Preproduction model of the downconverter-preamplifier assembly.

Combining the two filters into a single unit was within existing manufacturing and testing technology so that no mechanical development was needed. The two shorted waveguide sections on the horizontal arm of the filter in Fig. 13 are the resonance cavities of the bandstop filter. They are coupled to the horizontal waveguide by circular holes in the waveguide wall. A similar hole couples the lower of the two bandpass cavities in the vertical arm to the common port. The upper end of this cavity and both ends of the upper bandpass cavity are defined by triple-post obstacles. In manufacture, precise jigging is combined with differential soldering to achieve connections that are both electrically and mechanically reliable. Copper tuning screws permit compensation of manufacturing tolerances.

### 4.2 *Die-cast Housing*

The housing is assembled from two machined aluminum castings. The two halves, which are identical as raw castings, differ slightly in their final form because one half is machined to hold the collet assembly, while the other is machined to hold the coaxial LP filter and

the IF preamplifier. The housing was designed to be die-cast, although all preproduction models of the casting were made in plaster molds, which produce castings of quality similar to die casting at very reasonable cost for small runs or prototypes.

In order to use two identical castings, the housing had to be divided perpendicularly to the RF currents in the waveguide sidewalls. Particular care was taken in designing the mating surfaces in order to prevent RF leakage into or out of the assembly. The walls of the casting are 0.64 inch thick, but electrical contact is made on two 0.10-inch wide lands only. Clearance holes for the clamping screws are located between the two lands so that, on assembly, uniform and high contact pressure is assured on the inner land area. The cast-in clearance holes are spaced one inch apart around the periphery of the casting. With properly tightened 0.164 UNC screws, no RF interference was encountered even when the castings were slightly warped. (Some warping of the castings occurs during ejection from the die, even though generous drafts are provided on all noncritical surfaces.)

Good die castings have adequate dimensional accuracy and surface texture so that the inside of the housing and the peripheral lands do not have to be machined.

The assembly of the housing is straightforward. A cylindrical mandrel aligns the hole of the coaxial short with that of the coaxial LP filter. A rectangular mandrel aligns the WR-229 port. Fifteen hexagonal socket head screws are inserted through the cast-in holes into hexagonal nuts on the opposite side to clamp the assembly together. (A trough-like recess along the periphery of the castings prevents the nuts from turning during assembly.) At this point, the waveguide flange is drilled and finished in accordance with the Bell System standards for WR-229 waveguide flanges.

Die-casting alloy A360 was selected for the housing because it combines good corrosion resistance, castability, and strength with adequate electrical conductivity. Screws and nuts are made of zinc-plated carbon steel to reduce corrosion in humid climates.

### 4.3 *The Collet Assembly*

To be able to remove the diode without dismantling the modulator was an early design goal. Some sort of device was needed which would tightly grip one end of the diode and, when inserted into the modulator housing, plug the other end of the diode into a receptacle. Since the coaxial lowpass filter did not lend itself readily as the gripping

device, and since the IF preamplifier would have to be removed to gain access to the coaxial LPF, it was logical that the gripping device should be on the grounded end of the diode. This evolved into the collet assembly shown in Fig. 14.

The depth of collet insertion is limited by a 0.060-inch-thick shoulder in the housing. The inside diameter of the shoulder is the outside diameter of the previously-mentioned coaxial short, while the collet forms the inside diameter and the shorting plane. The shorting "plane" is actually a truncated cone. This not only assures that RF contact between the collet and the housing takes place at a well-defined diameter, that is, at the outside diameter of the short coaxial line, but it also reduces the likelihood of RF leakage into the receiver modulator from extraneous sources.

The collet is gold plated to reduce the dc contact resistance between diode and collet, as well as between collet and housing. The collet is designed to make cylindrical contact with the diode (rather than a circumferential line contact which, in the presence of friction, can lead to poor axial alignment of the diode in the collet).

A beam spring limits the axial force exerted by the collet assembly on the 0.060-inch thick shoulder in the housing. Experiments on a number of preproduction modulators indicated that a seating force of about 100 pounds is needed to prevent RF leakage.

The bending moment acting on the two screws which fasten the

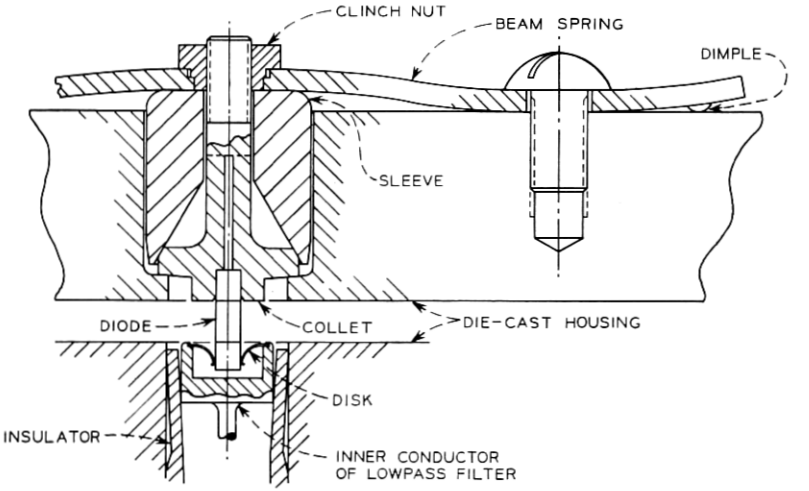


Fig. 14 — Diode mounting.

collet assembly to the housing is greatly reduced by dimpling the beam spring as shown in Fig. 14. Although the tensile force acting on the screws is thereby approximately doubled, the maximum stress in the screws is significantly reduced. Hard yellow brass was chosen for the beam spring because it combines adequate energy storage without heat treatment with good corrosion resistance, creep resistance, and sufficiently low hardness for pressing-in a commercial clinch nut. A nut that is integral with the beam spring guards against accidental release of the diode before the collet assembly is removed from the modulator.

### 4.4 *The Coaxial Lowpass Filter*

The coaxial lowpass filter consists of three parts, the outer conductor, insulator, and inner conductor (see Fig. 15.) As mentioned in Section 4.3, one end of the inner conductor has to serve as the diode receptacle. The major problem was designing this receptacle: how to make repeatable electrical contact between the diode and the filter without unduly stressing the relatively fragile diode. A more conventional problem concerned the positioning of the inner conductor in relation to the outer conductor (which is fastened to the housing) so that the diode receptacle would be flush with the waveguide wall and centered in its hole in the housing.

The second problem was solved by mechanically interlocking the injection-molded insulator and the inner conductor and then staking the combination in place through the wall of the outer conductor. Radial play between the diode receptacle and the waveguide wall is eliminated by a circumferential ridge (on the insulator), the diameter of which is somewhat larger than the hole in the modulator housing.

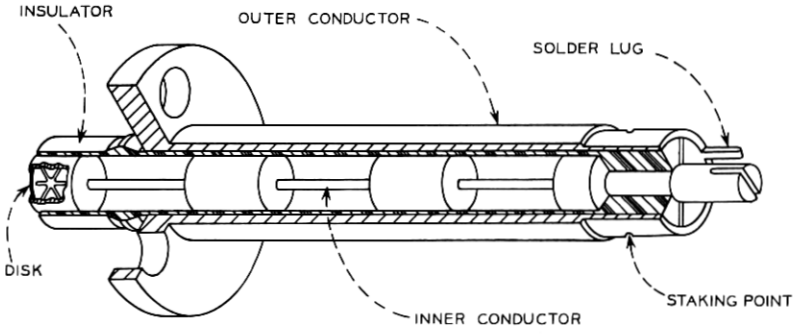


Fig. 15 — Coaxial lowpass filter.

A diametrical slot at each end of the insulator provides adequate radial compliance for both mechanical functions.

But designing a reliable diode receptacle was further complicated by the possibility of considerable diode misalignment from tolerance build-up in the collet assembly and from crookedness of the diode itself. After considering various alternatives, it was decided to attach a thin Beryllium-copper disk with six approximately triangular radial fingers (see Fig. 16) to the hollowed end of the inner conductor.

The constant-thickness finger is designed as a beam of uniform strength, that is, after a diode has been inserted, the maximum bending stress is the same in every cross section of the finger and hence its elastic deflection is at its greatest. The elastic deflection capability of the fingers is further increased by forming them after precipitation hardening rather than in the annealed state. It can be shown that the favorable residual stress distribution resulting from such a severe plastic deformation after hardening raises the elastic deformability by almost 50 per cent. The tips of the fingers are sharply bent to prevent them from digging into the diode during diode extraction.

It can be shown that the optimum number of radial fingers depends on the ratio of the width to the length of the radial slots separating the fingers. (The derivation is quite simple because of the constant-stress distribution in the fingers. Since we are interested in maximum elastic deformation of the fingers under a given load, we have to maximize the total potential energy stored in the disk. Since this is approximately proportional to the volume of the fingers, the optimum number of fingers is that which maximizes the volume of the fingers.) In general, the smaller the ratio of slot width to slot length, the greater are the optimum number of fingers and the elastic deforma-

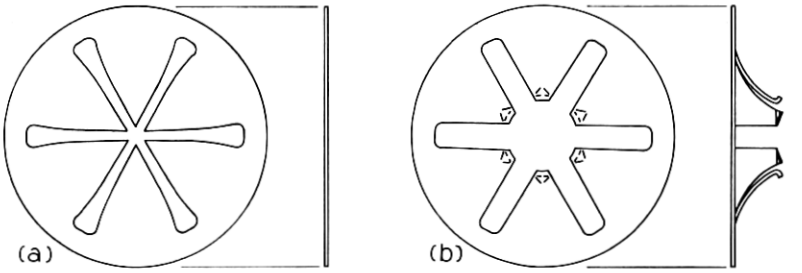


Fig. 16 — (a) The disk blank after photo etching. (b) The disk ready for installation after hardening and cold forming.

tion under a given load. We found a slot width of 0.010 inch necessary to assure separation of the fingers during manufacture. For this width and a 0.085-inch slot length, the theoretical optimum number of fingers is between 6 and 7.

The disk is photo-etched from 0.002-inch beryllium-copper foil. Its rim is clamped between an annular shoulder and a spun-over thin lip, both of which are part of the inner conductor (see Fig. 15). Both the inner and outer conductors are machined from free-cutting brass. The disk and the inner conductor are gold plated to minimize dc resistance.

The diode insertion force levels off at about ½ pound after many insertions and extractions. The contact resistance between simulated diodes and inner conductors was found to be about 1 milliohm. This is negligible in comparison with the series resistance $R_s$ of the diode which is typically 1 ohm.

## V. PERFORMANCE

### 5.1 *Local Oscillator Return Loss*

Figure 17 shows the local oscillator return loss of the converter block as discussed in item (*i*) of Section 3.2 (see Fig. 7). The measurement was made for three different diodes and in each case for three different bias currents, which were chosen to yield an optimum local oscillator match at $f_{LO}$ = 3780, 3940, and 4100 MHz. The maximum local oscillator power of $P_{LO}$ = 6 dBm was used, since it yielded the lowest $CL$. It is evident that a rather good broadband match can be achieved for each diode around any local oscillator frequency between 3780 and 4120 MHz.

It was found that the total capacitance $C_{TO}$ of the diode at zero bias is virtually the only characteristic of the diode which affects the bias current required for an optimum match at a given local oscillator frequency; as a consequence, diodes with equal $C_{TO}$ require practically identical bias currents.

The diode specification[9] calls for 0.30 pF $\leqq C_{TO} \leqq$ 0.60 pF. Therefore, Fig. 17 with $C_{TO}$ = 0.31, 0.45, and 0.61 pF is quite representative of the range of $C_{TO}$ that will be available. It can, therefore, be concluded from Fig. 17 that the local oscillator return loss of the converter block is above 15 dB for any diode and for any local oscillator frequency between 3780 and 4120 MHz after proper adjustment of the bias current. Since the return loss at port 2 of the directional filter (Figs. 4 and 5) is well above 20 dB, the return loss $RL_{LO}$ at $f_{LO}$ of the downconverter-

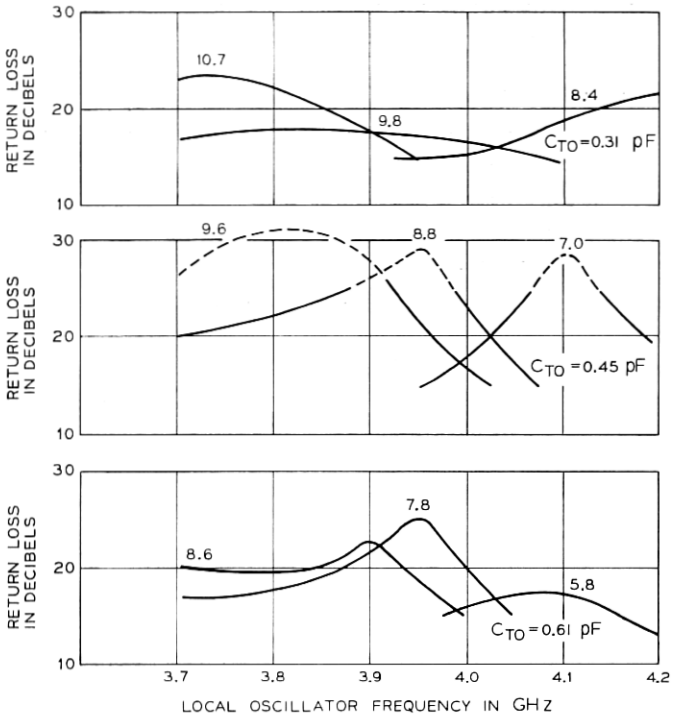


Fig. 17 — Measured local oscillator return loss of the converter block. (Diode bias current in mA.)

preamplifier unit at its local oscillator input port (Fig. 3) is well above the specified value of 10 dB, typically > 15 dB.

It was also found that the incremental change in bias current needed to shift the optimum local oscillator return loss point from one local oscillator frequency to another is practically independent of the diode and approximately linearly related to the frequency difference. To a good approximation, the bias current, $I$, required for an optimum match at $f_{LO}$ can be obtained from:

$$I(f_{LO}) = I(3940 \text{ MHz}) - 1.2 \text{ mA} \frac{f_{LO}/\text{MHz} - 3940}{340}. \quad (5)$$

Finally, it was determined that, in order to remain at the point of optimum local oscillator match with varying local oscillator power, the bias current should be kept constant. In practice this was realized

to a good approximation by biasing the diode from the available voltage of −19 V through a series resistor.

### 5.2 *IF Output Impedance*

Figure 18 shows the IF output impedance $Z_{IFout}$ discussed in (*ii*) of Section 3.2 for the three diodes mentioned in Section 5.1. $Z_{IFout}$ is fairly independent of the particular diode and local oscillator frequency, and it is approximately real and constant from 60 to 80 MHz. The mean value is:

$$Z_{IFout} = 58\Omega - j16\Omega. \tag{6}$$

### 5.3 *Transmission Characteristics*

Figure 19 shows a typical signal-to-IF amplitude transmission characteristic of the downconverter as discussed in (*iii*) of Section 3.2.

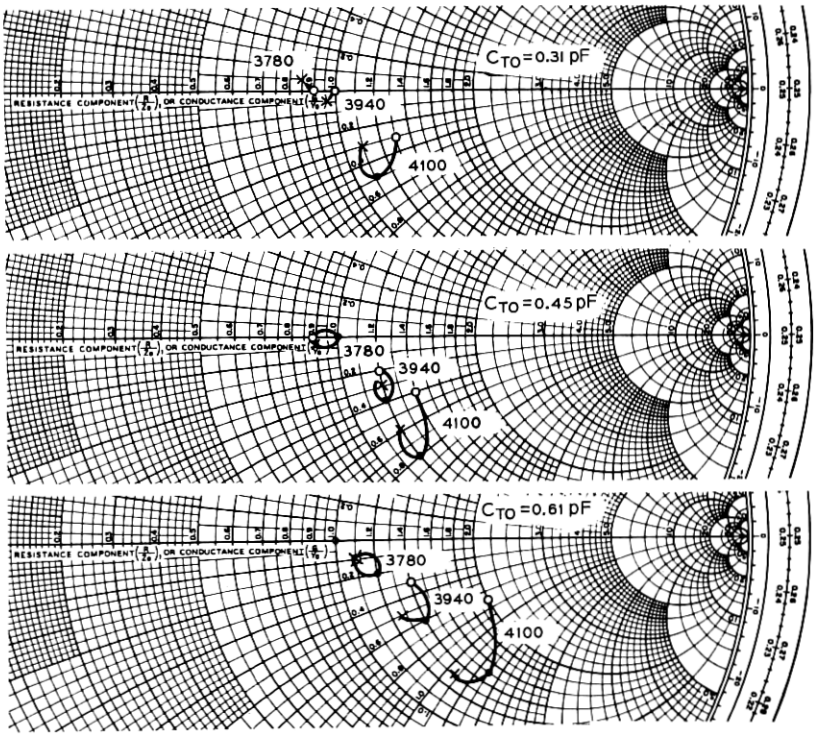


Fig. 18 — Measured IF output impedance of the downconverter.

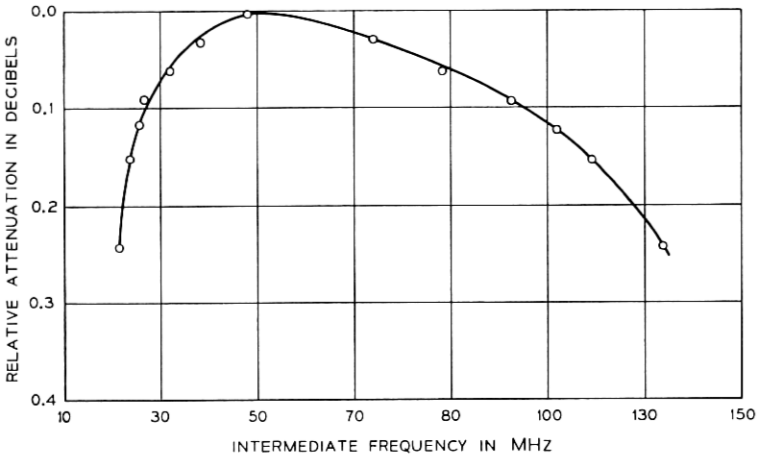


Fig. 19 — Measured signal-to-IF amplifier transmission characteristic of the downconverter.

Because of the availability of test equipment, the IF load $R_{IF}$, which shall approximately equal $Z_{IFout}$ as explained in Section 3.2, was chosen to be:

$$R_{IF} = 50\Omega. \tag{7}$$

A typical conversion loss $CL$ at 70 MHz is:

$$CL = 4.2 \text{ dB}. \tag{8}$$

Figure 19 shows that the signal-to-IF amplitude transmission characteristic of the downconverter typically exhibits a slope of 0.03 dB per 20 MHz from 60 to 80 MHz, which is definitely small enough to be corrected in the IF preamplifier.

Figure 20 shows a typical signal-to-IF amplitude transmission characteristic of the downconverter-preamplifier unit (Fig. 3) after properly adjusting the two transmission amplitude controls and the output level control of the preamplifier. The specifications for transmission amplitude flatness (indicated tolerance field) are met with ample margin. However, notice that although the response of Fig. 20 is quite flat, it is considerably narrower than that of Fig. 19 because of the bandpass characteristic of the IF preamplifier.

### 5.4 *Noise Figure*

For various signal and local oscillator frequencies, Fig. 21 shows the median total noise figure $NF_{Total}$ of a downconverter-preamplifier

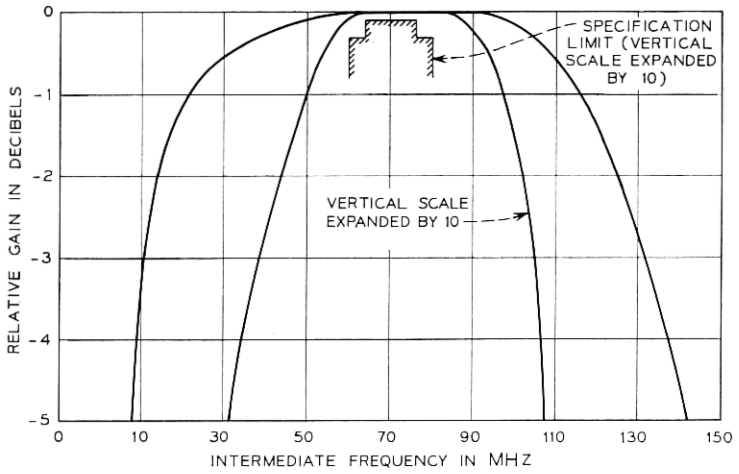


Fig. 20 — Measured signal-to-IF amplitude transmission characteristic of the downconverter-preamplifier unit.

unit (Fig. 3) obtained from a sample of 97 diodes. The noise figure is lowest near the center of the band, and rises by 0.1 and 0.3 dB at the low and the high end of the band, respectively. The noise figure of the IF preamplifier, $NF_{IF}$ as defined in Section 3.2, was in this case:

$$NF_{IF} = 2.8 \text{ dB} \tag{9}$$

measured from $R_{IF} = 50\Omega$.

It must be pointed out here, that as mentioned in Ref. 10, the input impedance of the IF preamplifier is *not* equal to $R_{IF} = 50\Omega$, contrary to the assumption made in (*iv*) of Section 3.2. Hence, equation (4) cannot be expected to give the relationship between a typical $NF_{Total}$ of Fig. 21 and $CL$ and $NF_{IF}$ of equations (8) and (9), respectively, since $CL$ is measured with $R_{IF} = 50\Omega$ as load impedance.

The diode specification[9] calls for a maximum total noise of 7.3 dB for the downconverter-preamplifier unit with $NF_{IF} = 2.8$ dB and at $f_{SI} = 3950$ MHz. (The isolator with an insertion loss of approximately 0.2 dB is excluded). The IF preamplifier specification limits $NF_{IF}$ to 3.0 dB maximum. Thus the total noise figure is limited to 8.0 dB maximum at the limits of the band (7.5 dB + 0.3 dB degradation at the high end of the band + 0.2 db from the isolator), which meets the requirement of < 8.0 dB. However, the average result for 49 pre-production models was $NF_{Total} = 6.7$ dB (isolator excluded).

### 5.5 *Compression Characteristics*

Figure 22 shows the compression characteristic of the downconverter-preamplifier unit. It is seen that the break point of the downconverter is remarkably high ($P_{si} = -4$ dBm) considering that $P_{LO} = 6$ dBm. The compression characteristic of the downconverter-preamplifier unit is clearly determined by the preamplifier.

### 5.6 *Level of Unwanted Signals*

The results of a test made on a downconverter-preamplifier unit are:

Local oscillator suppression from the local oscillator port to:
(*i*) the signal port: 89 dB.
(*ii*) the IF preamplifier input: 65 dB.
Level of the second harmonic of the local oscillator at:
(*iii*) the signal port: more than 76 dB below $P_{LO}$.
(*iv*) the IF preamplifier input: more than 76 dB below $P_{LO}$.
Level of the third harmonic of the local oscillator at:
(*v*) the signal port: more than 51 dB below $P_{LO}$.
(*vi*) the IF preamplifier input: more than 38 dB below $P_{LO}$.
RF leakage:
(*vii*) satisfactorily low.

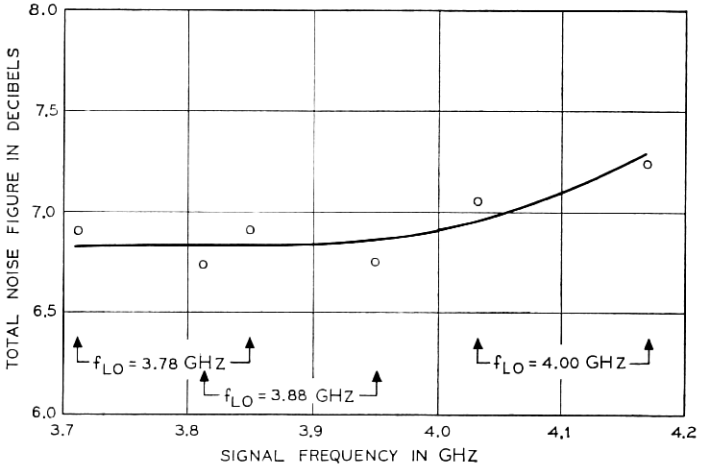


Fig. 21 — Median measured total noise figure of a downconverter-preamplifier unit for 97 diodes.

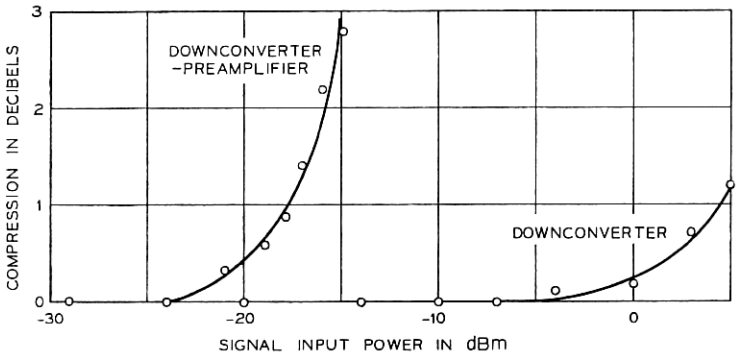


Fig. 22 — Measured compression characteristics of the downconverter and the downconverter-preamplifier unit.

Thus all requirements have been met with ample margin, except possibly for (*vi*). However, it can be expected that there will be at least 2 dB of attenuation between the input and output of the IF preamplifier for the third harmonic of the local oscillator frequency.

### 5.7 *Temperature Behavior*

A temperature test of a preproduction downconverter-preamplifier unit (Fig. 3) gave the following results:

| Temperature (°F): | 40 | 70 | 80 | 90 | 140 |
|---|---|---|---|---|---|
| Local oscillator suppression from local oscillator port to signal port without isolator (dB): | 29 | — | 51 | — | 28 |
| Slope of the transmission characteristic from signal to IF (dB per 12 MHz): | 0.04 | 0.01 | 0 | −0.02 | −0.16 |

These results show that the local oscillator suppression from the local oscillator port to the signal port stays well above the required 5 dB. The results also show that the amplitude transmission characteristic from signal to IF (0.01 dB per 12 MHz) is slightly more sensitive to temperature within the ±10°F range, than would be desired. This, however, is not expected to impair the performance of the system noticeably. Performance at the extreme temperatures is such that the system will still be able to render a good service, as required.

## APPENDIX

It is the purpose of the Appendix to show that the noise performance of a single-diode downconverter is identical to that of a balanced downconverter, if the noise of the local oscillator is properly band limited.

The diode is modeled as a memoryless, frequency independent, quadratic scatterer with a built-in noise source:

$$b(t) = A_1 a(t) + A_2 a^2(t) + b_N(t).$$

$a(t)$ is the incident wave, $b(t)$ is the reflected wave, $b_N(t)$ is that portion of $b(t)$ which results from the built-in noise source. All waves are normalized to a reference impedance $R$. $A_1$ and $A_2$ are real constants. For a linear network, $A_1$ would be called the reflection coefficient.

To study the performance of this diode model in a single-diode downconverter, the converter is modeled as shown in Fig. 23. The "ideal multiplexer" is a lossless network with the following scattering matrix.

$$\begin{vmatrix} b_1 \\ b_2 \\ b_3 \\ b_4 \\ b_5 \\ b_6 \end{vmatrix} = \begin{vmatrix} S_{11} & 0 & 0 & 0 & 0 & S_{16} \\ 0 & S_{22} & 0 & 0 & 0 & S_{26} \\ 0 & 0 & S_{33} & 0 & 0 & S_{36} \\ 0 & 0 & 0 & S_{44} & 0 & S_{46} \\ 0 & 0 & 0 & 0 & S_{55} & S_{56} \\ S_{16} & S_{26} & S_{36} & S_{46} & S_{56} & 0 \end{vmatrix} \cdot \begin{vmatrix} a_1 \\ a_2 \\ a_3 \\ a_4 \\ a_5 \\ a_6 \end{vmatrix}$$

The nonzero elements of this matrix have the following values as a function of frequency:

(*i*) $S_{ii} = 0$ for the frequency range $B_i$, otherwise $|S_{ii}| = 1$.
(*ii*) $S_{i6} = 1$ for the frequency range $B_i$, otherwise $S_{i6} = 0$.
(*iii*) The five $B_i$ ($i$=1, 2, 3, 4 and 5) are defined as:

$B_1$: $0 \leq \omega \leq 2\alpha$

$B_2$: $\omega_2 - 2\alpha \leq \omega \leq \omega_2 + 2\alpha$

$B_3$: $\omega_3 - 2\alpha \leq \omega \leq \omega_3 + 2\alpha$

$B_4$: $\omega_3 - \omega_2 - 2\alpha \leq \omega \leq \omega_3 - \omega_2 + 2\alpha$

$\omega_3 + \omega_2 - 2\alpha \leq \omega \leq \omega_3 + \omega_2 + 2\alpha$

$B_5$: All other $\omega$.

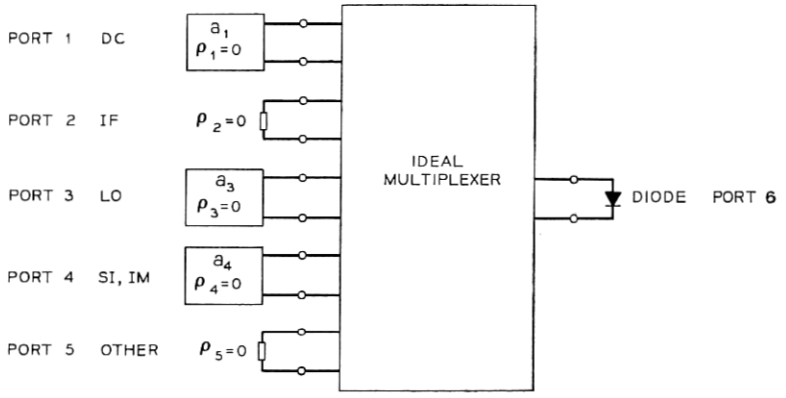


Fig. 23 — Model of a single-diode downconverter.

Here $\omega_3$ denotes the frequency of the local oscillator carrier, $(\omega_3 \pm \omega_2)$ the frequency of the signal carrier and the image carrier, respectively, and and $\omega_2$ the frequency of the IF carrier. This also explains the nomenclature used at ports 1 through 5 (dc, IF, and so on). The frequency $\alpha$ is restricted to $\alpha < \omega_2/4$, otherwise arbitrary.

As shown in Fig. 23, ports 1 through 5 are terminated in sources or loads. All are matched $(\rho_i=0)$ and the source waves are:

$$a_1(t) = a_1$$

$$a_3(t) = a_3[1 + m_3(t)] \cos [\omega_3 t + \varphi_3(t) + \psi_3]$$

$$a_4(t) = a_4[1 + m_4(t)] \cos [\omega_3 t + \omega_2 t + \varphi_4(t) + \psi_4]$$

$a_1$, $a_3$, $a_4$, $\psi_3$, $\psi_4$ are real constants, $m_3(t)$, $\varphi_3(t)$ describe AM and PM noise impressed on the local oscillator carrier, and $m_4(t)$, $\varphi_4(t)$ describe AM and PM noise or modulation impressed on the signal carrier. It is assumed that the spectra of $m_3(t)$ and $m_4(t)$ are limited to the frequency range $\pm\alpha/2$, and that the spectra of cos $[\omega_3 t + \varphi_3(t) + \psi_3]$ and cos $[\omega_3 t + \omega_2 t + \varphi_4(t) + \psi_4]$ are limited to the frequency ranges $\omega_3 \pm \alpha/2$ and $\omega_3 + \omega_2 \pm \alpha/2$, respectively.

Hence, the spectra of $a_3(t)$ and $a_4(t)$ are limited to the frequency ranges $\omega_3 \pm \alpha$ and $\omega_3 + \omega_2 \pm \alpha$, respectively. It should be remembered that, in addition to $a_1(t)$, $a_3(t)$ and $a_4(t)$, white thermal noise is delivered to the ideal multiplexer at ports 1 through 5 from each of the matches presented to the multiplexer at these ports. These incident noise waves are denoted by $a_{N1}(t)$, $a_{N2}(t)$, and so on.

The wave incident to the diode at port 6 can then be calculated:

$$a(t) = a_1(t) + a_3(t) + a_4(t) + a_N(t)$$

where $a_N(t)$ represents the white thermal noise wave incident to the diode from the match which the multiplexer presents to the diode. Obviously it is:

$$a_N(t) = a_{N1}(t)_{B_1} + a_{N2}(t)_{B_2} + a_{N3}(t)_{B_3} + a_{N4}(t)_{B_4} + a_{N5}(t)_{B_5}$$

where the subscripts indicate that only the components falling within the respective frequency range are to be taken. If it is now assumed that:

$$a_4 , a_N(t) \ll a_1 , a_3$$

the wave reflected from the diode can readily be calculated. In particular, the wave $b_2(t)$ incident to the load at port 2 (*IF*) is:

$$\begin{aligned} b_2(t) = {} & A_2a_3a_4[1 + m_3(t)][1 + m_4(t)] \cos [\omega_2 t + \varphi_4(t) - \varphi_3(t) + \psi_4 - \psi_3] \\ & + \langle A_1a_N(t) + b_N(t) + 2A_2a_1a_N(t) + 2A_2a_3[1 + m_3(t)] \\ & \cdot a_N(t) \cos [\omega_3 t + \varphi_3(t) + \psi_3]\rangle_{B_2} \\ = {} & A_2a_3a_4[1 + m_3(t)][1 + m_4(t)] \cos [\omega_2 t + \varphi_4(t) - \varphi_3(t) + \psi_4 - \psi_3] \\ & + (A_1 + 2A_2a_1)a_{N2}(t)_{B_2} + b_N(t)_{B_2} \\ & + \langle 2A_2a_3[1 + m_3(t)] \cos [\omega_3 t + \varphi_3(t) + \psi_3]a_{N4}(t)_{B_4}\rangle_{B_2} . \end{aligned}$$

To study the performance of the same diode model when used in a balanced downconverter, the converter is modeled as shown in Fig. 24.

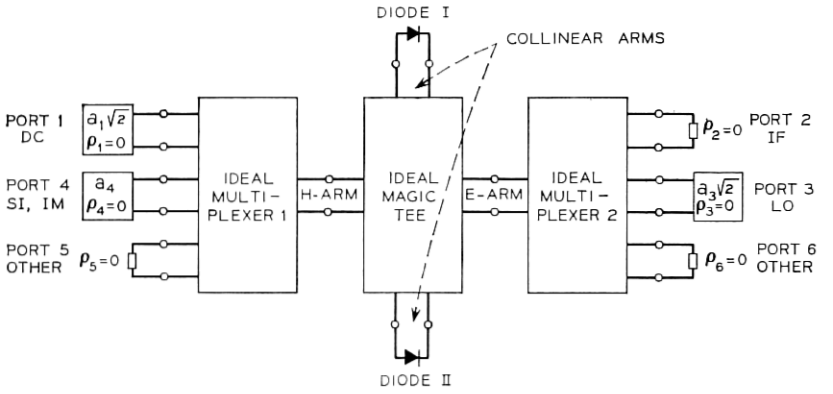


Fig. 24 — Model of a balanced downconverter.

The ideal tee hybrid is a lossless hybrid matched at all four ports. It has infinite isolation, and the transmission coefficients are $2^{-\frac{1}{2}}$ from the H-arm to both collinear arms and $\pm 2^{-\frac{1}{2}}$ from the E-arms to the top (diode I) and bottom (diode II) collinear arm, respectively. The two ideal multiplexers have properties analogous to those outlined for the ideal multiplexer of Fig. 23.

Notice that the signal source at port 4 remained unaltered in strength (since this can commonly not be changed), but that the power of both the DC and LO source have been increased by a factor of 2 (wave amplitudes increased $2^{\frac{1}{2}}$) in order to provide the same DC and LO power to each diode as before for the single diode.

The wave incident to diode $I$ is then:

$$a_I(t) = a_1(t) + a_3(t) + 2^{-\frac{1}{2}}a_4(t) + 2^{-\frac{1}{2}} \cdot [a_{N1}(t)_{B_1} + a_{N4}(t)_{B_4} + a_{N5}(t)_{B_5} + a_{N2}(t)_{B_2} + a_{N3}(t)_{B_3} + a_{N6}(t)_{B_6}]$$

and the wave incident to diode $II$ is:

$$A_{II}(t) = a_1(t) - a_3(t) + 2^{-\frac{1}{2}}a_4(t) + 2^{-\frac{1}{2}} \cdot [a_{N1}(t)_{B_1} + a_{N4}(t)_{B_4} + a_{N5}(t)_{B_5} - a_{N2}(t)_{B_2} - a_{N3}(t)_{B_3} - a_{N6}(t)_{B_6}].$$

The resulting wave $b_2(t)$ incident to the load at port 2 (IF) is now:

$$\begin{aligned} b_2(t) = {} & A_2a_3a_4[1 + m_3(t)][1 + m_4(t)] \cos [\omega_2 t + \varphi_4(t) - \varphi_3(t) + \psi_4 - \psi_3] \\ & + \langle A_1[a_{N2}(t)_{B_2} + a_{N3}(t)_{B_3} + a_{N6}(t)_{B_6}] + 2^{-\frac{1}{2}}[b_{NI}(t) - b_{NII}(t)] \\ & + 2A_2a_1[a_{N2}(t)_{B_2} + a_{N3}(t)_{B_3} + a_{N6}(t)_{B_6}] + 2A_2a_3[1 + m_3(t)] \\ & \cdot [a_{N1}(t)_{B_1} + a_{N4}(t)_{B_4} + a_{N5}(t)_{B_5}] \cos [\omega_3 t + \varphi_3(t) + \psi_3]\rangle_{B_2} \\ = {} & A_2a_3a_4[1 + m_3(t)][1 + m_4(t)] \cos [\omega_2 t + \varphi_4(t) - \varphi_3(t) + \psi_4 - \psi_3] \\ & + (A_1 + 2A_2a_1)a_{N2}(t)_{B_2} + 2^{-\frac{1}{2}}[b_{NI}(t) - b_{NII}(t)]_{B_2} \\ & + \langle 2A_2a_3[1 + m_3(t)] \cos [\omega_3 t + \varphi_3(t) + \psi_3]a_{N4}(t)_{B_4}\rangle_{B_2} . \end{aligned}$$

$b_{NI}(t)$ and $b_{NII}(t)$ are the built-in noise waves of diode I and diode II, respectively.

Since $b_{NI}(t)$ and $b_{NII}(t)$ are uncorrelated and represent the same noise as $b_N(t)$ for the unbalanced downconverter, it is seen that $b_2(t)$ is equal for the balanced and the single-diode downconverter. As can be seen by going through the detailed analysis, this is a consequence of the fact that the spectra of $m_3(t)$ and $a_3(t)$ are limited to the frequency ranges $\pm \alpha/2$ and $\omega_3 \pm \alpha$, respectively, and that $\alpha < \omega_2/4$.

REFERENCES

1. Hathaway, W. D., Hensel, W. G., Jordan, D. R., and Prime, R. C., "Radio System," this issue, pp. 1143–1188.
2. Abele, T. A., A High-Quality Waveguide Directional Filter," B.S.T.J., *46*, No. 1 (January 1967), pp. 81–104.
3. Cohn, S. B., "Analysis of a Wideband Waveguide Filter," Proc. IEEE, *37*, No. 6 (June 1949), pp. 651–656.
4. Drazy, E. J., MacLean, R. C., Sheehey, R. E., "Networks," this issue, pp. 1397–1422.
5. Barber, M. R., "Noise Figure and Conversion Loss of the Schottky Barrier Mixer Diode," IEEE Trans. Microwave Theory and Techniques, *MTT-15*, No. 11 (November 1967), pp. 629–635.
6. Young, L., "Stepped-Impedance Transformers and Filter Prototypes, "IEEE Trans. Microwave Theory and Techniques, *MTT-10*, No. 9 (September 1962), pp. 399–359.
7. Young, L., "Postscript to Two Papers on Waffle-Iron Filters," IEEE Trans. Microwave Theory and Techniques, *MTT-11*, No. 11 (November 1963), pp. 555–557.
8. Radio Research Laboratory Staff, Harvard University, *Very High Frequency Techniques*, vol. II, Chapter 27, New York: McGraw-Hill, 1947,
9. Elder, H. E., and others, "Active Solid-State Devices," B.S.T.J., this issue, pp. 1323–1377.
10. Fenderson, G. L., Jansen, J. J., and Lee, S. H., "Active IF Units for the Transmitter and Receiver," B.S.T.J., this issue, pp. 1227–1256.